SLAC-PUB-1624
August 1975
(T/E)

e^+e^- ANNIHILATION INTO HADRONS AT SPEAR*

G. J. Feldman
Stanford Linear Accelerator Center, Stanford, California 94305, USA.

1. INTRODUCTION

My charge was to review e^+e^- annihilation into hadrons excluding the new particles. I will interpret this last phrase liberally and consider anything which Dr. Lüth did not cover as fair game.

I will briefly review the detectors which have been used at SPEAR and then discuss the total hadronic cross sections, the charged multiplicity, and inclusive distributions. I will conclude with some results on the search for new particles at SPEAR: searches for monochromatic photons from the ψ', a search for nonleptonic decays of charmed mesons, and evidence for anomalous lepton production.

2. DETECTORS

The bulk of the data in this report come from the SLAC-LBL magnetic detector[1] which is shown in Fig. 1. Dr. Lüth has already described this detector in some detail,[2] so I will just point out some of the features which will be relevant for this report. The detector has a solenoidal coil which

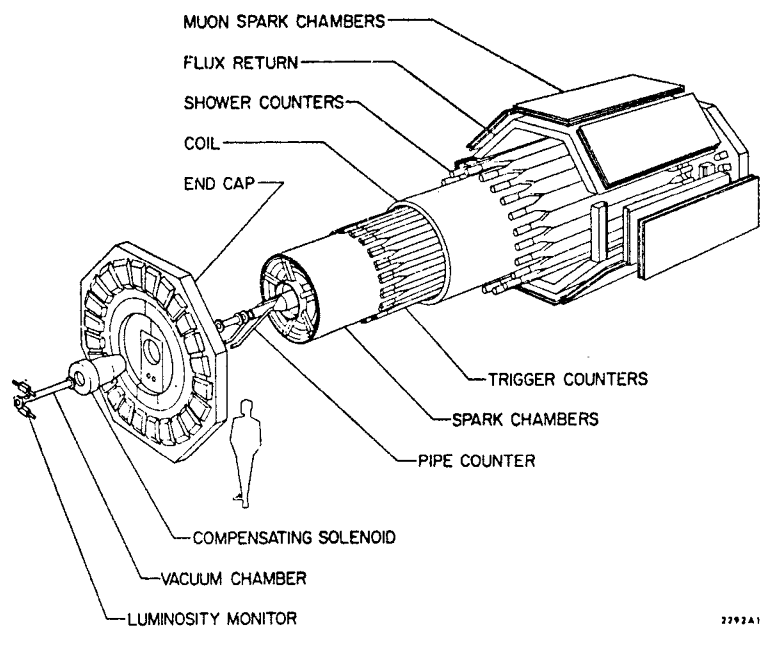

Fig. 1 Telescoped view of the SLAC-LBL magnetic detector.

produces a magnetic field parallel to the incident beams. A set of cylindrical spark chambers measures trajectories of charged particles over about 70% of the full solid angle. The trigger for an event is two or more charged particles which each fire a trigger and shower counter. The counters cover about 65% of the solid angle. Separation of π's, K's, and p's is accomplished by time-of-flight measurements in the trigger counters. π-K separation is possible up to momenta of about 700 MeV/c

*) Work supported by the U.S. Energy Research and Development Administration and by a U.S. National Science Foundation International Travel Grant.

(Rapporteur talk at the International Conference on High Energy Physics, Palermo, Italy, 23-28 June 1975)

and K-p separation is possible to momenta of about 1 GeV/c. Electrons can be identified as particles which cause large pulse heights in the shower counters and muons can be identified as particles which penetrate the flux return and fire the muon spark chambers.

I will also report on results of two experiments which were situated in the other interaction region of SPEAR. The apparatus of a Princeton-Pavia-Maryland experiment is shown in Fig. 2. The important feature of this experiment was a gas Cerenkov counter followed by a magnet, which provided particle separation at high momenta.

Figure 3 shows the apparatus of a Stanford experiment. The main purpose of the experiment was to study quantum electrodynamics. However, the large NaI crystals were also useful to search for monochromatic photons from ψ' decay, and it is on this aspect of the experiment that I will report.

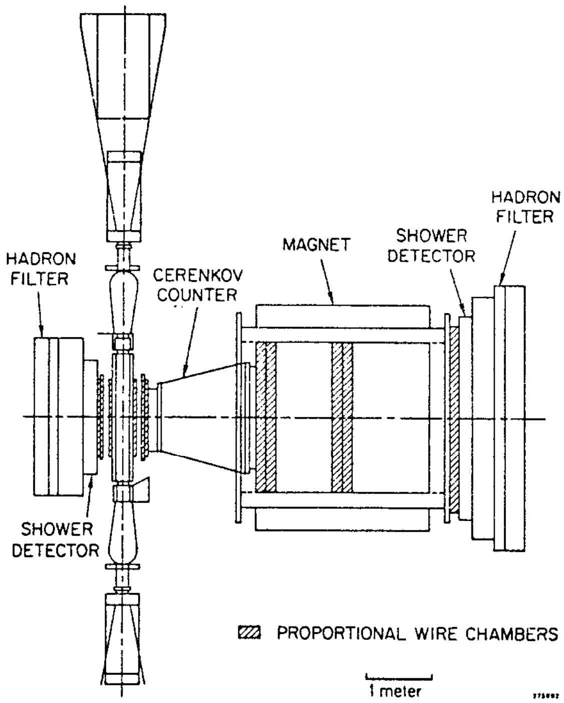

Fig. 2 Princeton-Pavia-Maryland experimental apparatus viewed from above.

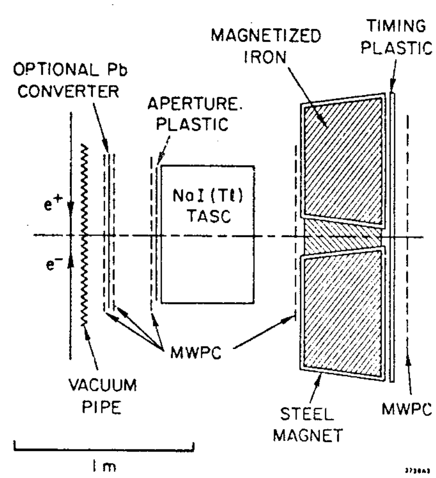

Fig. 3 One of the two NaI crystal spectrometers of the Stanford experiment.

3. TOTAL HADRONIC CROSS SECTIONS

The event sample used in determining the total cross section by the SLAC-LBL magnetic detector includes events with three or more observed charged particles and events with two observed charged particles in which the two particles satisfy two conditions: (a) that their coplanarity angle with the incident beam is greater than 20° and (b) that both particles have momenta greater than 300 MeV/c. These two conditions are necessary to eliminate backgrounds from one and two photon leptonic events.

Corrections must be made for tracking losses, beam-gas interactions, two photon-leptonic events, and radiative effects. These corrections are relatively straightforward. The correction for triggering efficiency is not so straightforward. To calculate this, we must construct a model of the final state and perform a Monte Carlo simulation. In this way our imperfect knowledge of the final state leads to a 10 to 15% uncertainty in the absolute value of the total cross sections.[3)]

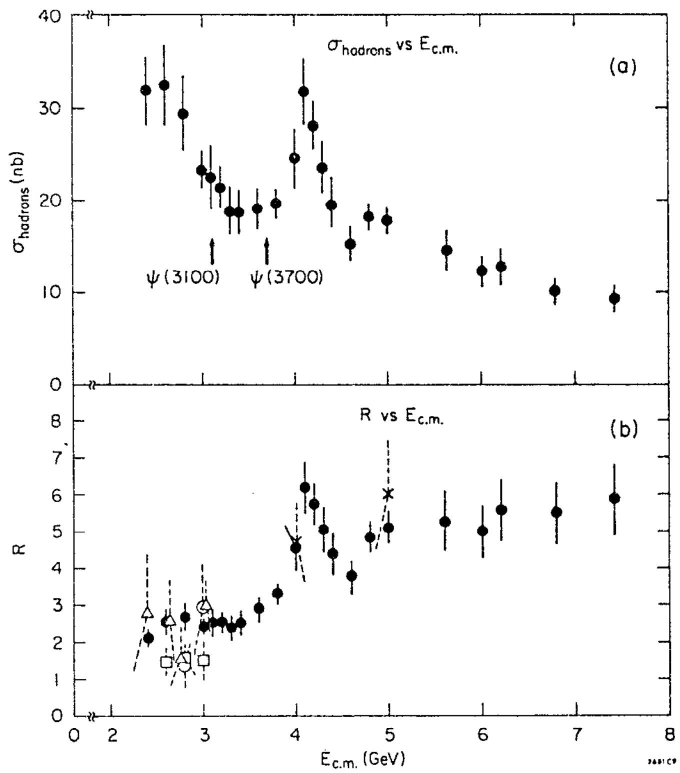

Fig. 4 a) The total hadronic cross section versus center-of-mass energy.
b) The ratio R of the total hadronic cross section to the theoretical muon pair production cross section. The dotted points are older results from Frascati and the CEA.

I emphasize this point in order to warn you not to take the absolute values of the cross sections too literally.

Figure 4a shows the total hadronic cross section as a function of center-of-mass energy and Fig. 4b shows the ratio R of the total cross section to the μ pair production cross section. The data through 5 GeV have been published[4)] while the data from 5.6 GeV through 7.4 GeV are new preliminary results. The positions of the ψ and ψ' are indicated by arrows. On the scale of this plot, they are infinitesimally narrow spikes.

There are two regions where R appears to be constant - below 3.5 GeV where $R \approx 2.5$ and above 4.8 GeV where $R \approx 5.5$. In a quark-parton model R is just the sum of the squares of the quarks. Thus the two plateaus in R suggest that new quarks are being coupled to at the higher energies and that, correspondingly, new particle states are being produced.

There is an enhancement around 4.1 GeV which is probably a resonance, but might possibly be a threshold enhancement. We presently have little experimental information about this region, but we are currently acquiring more data.

4. CHARGED MULTIPLICITY

Figure 5 shows the mean charged multiplicity as a function of c.m. energy, which is plotted on a logarithmic scale. This is an "experimenter's multiplicity"; for example, on the average a K_S^0 is counted as 1.4 charged particles. The errors shown are only the statistical errors. Note the high statistics points at 3.0, 3.8, and 4.8 GeV. Within errors all of the data lie on a straight line corresponding to a multiplicity which is proportional to ln s. In particular, there is no evidence for any change of slope in

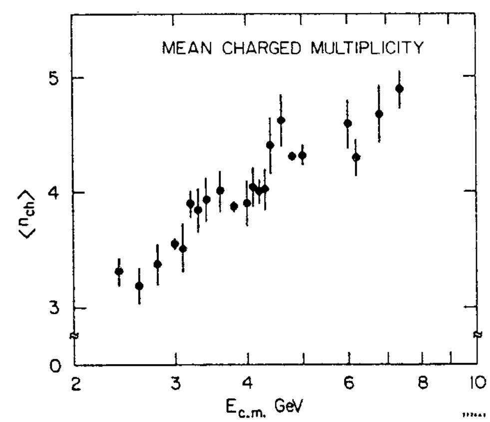

Fig. 5 The mean charged multiplicity versus center-of-mass energy.

the transition region between the two plateaus in R.

5. INCLUSIVE DISTRIBUTIONS

5.1 Momentum distributions

Although I was originally planning to show some momentum distributions, I will not do so today in order to generate some time for more exciting results. I will simply apologize for the current state of our inclusive distributions. Back before we knew how the land lay, we chose c.m. energies 3.0, 3.8, and 4.8 GeV to do detailed studies of inclusive distributions. With hindsight, we can now see that we could not have picked three worse energies at which to study scaling. One is in the lower plateau region, one is in the upper plateau region, and the third is in the transition region and heavily contaminated by the tail of the ψ'. New studies of the inclusive distributions are in progress and some results should be ready by the Photon Conference. The old results were presented at the London Conference; I refer you to those Proceedings for them.[5)]

5.2 Polarization and angular distributions

We have an exciting new result from the SLAC-LBL magnetic detector on the inclusive angular distributions which is now barely two weeks old. In a nutshell, we have observed that the e^+e^- beams are polarized at a c.m. energy of 7.4 GeV and that high momentum hadrons develop an azimuthal distribution which is similar to that developed by μ pairs.

It has been realized for a long time that, in the absence of depolarizing effects, electrons and positrons in a storage ring would become polarized antiparallel and parallel to the magnetic guide field.[6)] The polarization builds up exponentially in time

$$P(t) = P_0(1 - e^{-t/\tau}) \tag{1}$$

where P_0 is the maximum polarization, theoretically $P_0 = .924$. The characteristic time τ is machine-dependent and is a strong function of the c.m. energy, E:

$$\tau_{\text{SPEAR}} = \frac{5280}{E^5} \text{ hours} \tag{2}$$

where E is measured in GeV. Eq. (2) is evaluated for several energies in Table I. Since we normally refill the rings every two to three hours, there is almost no polarization at the ψ's, only a small amount at 4.8 GeV, but very high average polarization at 7.4 GeV.

TABLE 1

Calculated Polarization Time at SPEAR

$E_{c.m.}$	τ
ψ	18 hours
ψ'	$7\frac{1}{2}$ hours
4.8 GeV	2 hours
7.4 GeV	14 minutes

Under the assumption of one photon exchange, the inclusive angular distributions are of the following form:[7)]

$$\frac{d\sigma}{d\Omega} = (\sigma_T + \sigma_S) + (\sigma_T - \sigma_S)\cos^2\theta + $$
$$+ P^2(\sigma_T - \sigma_S)\sin^2\theta \cos 2\phi \tag{3}$$

where θ and ϕ are the polar and azimuthal angles and where ϕ is taken to be zero in the plane of the ring. The important thing to note about Eq. (3) is that there are only two parameters, σ_T and σ_S, which are functions of c.m. energy and the momentum of the detected hadron. These parameters can clearly be measured even if the polarization were zero. Therefore the polarization gives us no new theoretical information. However, since the detector measures only a portion of the θ region, but is almost completely unbiased in ϕ, the polarization is extremely important experimentally.

To illustrate Eq. (3), we'll take two examples: If we produce a pair of point spin $\frac{1}{2}$ particles such as μ's, and ignore their mass, $\sigma_T = 0$. If we average over ϕ or have no polarization, then

$$\frac{d\sigma}{d\Omega} \propto 1 + \cos^2\theta \ . \tag{4a}$$

On the other hand, if we take the somewhat unphysical case of 100% polarization and look around $\theta = 90^o$, then

$$\frac{d\sigma}{d\Omega} \propto 1 + \cos 2\phi \ . \tag{4b}$$

For the case of a produced pair of spin 0 particles, Eqs. (4a) and (4b) become

$$\frac{d\sigma}{d\Omega} \propto \sin^2\theta \tag{5a}$$

and

$$\frac{d\sigma}{d\Omega} \propto 1 - \cos 2\phi \ . \tag{5b}$$

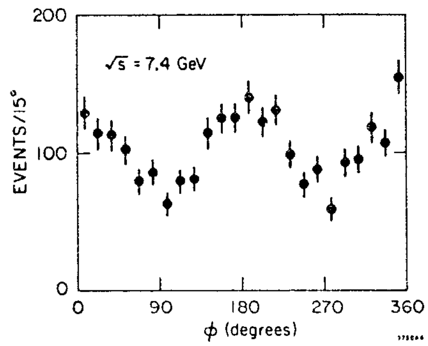

Fig. 6 Preliminary results for the azimuthal distribution of observed hadrons with $x \equiv 2p/\sqrt{s} > 0.3$ at 7.4 GeV center-of-mass energy.

Figure 6 shows the azimuthal angle distribution for high momentum hadrons observed in the detector. The distribution shows a clear azimuthal dependence of the type expected for μ pairs. Figure 7 shows the quantity $(\sigma_T - \sigma_S)/(\sigma_T + \sigma_S)$ as a function of x ($x = 2p/E_{c.m.}$). At low x, $\sigma_T \approx \sigma_S$, which corresponds to an isotropic distribution, but at higher x, $\sigma_T >> \sigma_S$.

These results agree with an old prediction of the spin $\frac{1}{2}$ parton model - that leading particles should have the same distribution as μ pairs. Of course the data do not prove that the parton description is correct; but it is significant that they occur in the manner predicted by the model.

Even more interesting is that we have found evidence for jet structure in the 7.4 GeV data. In each event we find the axis to which the sum of squares of the transverse momenta of all the particles is a minimum. We then compare these transverse momenta to those predicted by an isotropic phase space Monte Carlo simulation and find that on the average they are significantly smaller. Further, the jet axis shows the same azimuthal dependence as the high energy hadrons. We are presently putting these results into quantitative form.

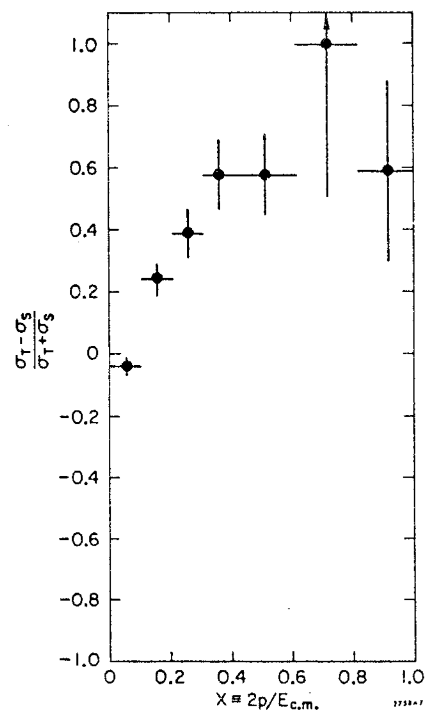

Fig. 7 Preliminary results for $(\sigma_T - \sigma_S)/(\sigma_T + \sigma_S)$ versus $x \equiv 2p/\sqrt{s}$ at 7.4 GeV center-of-mass energy.

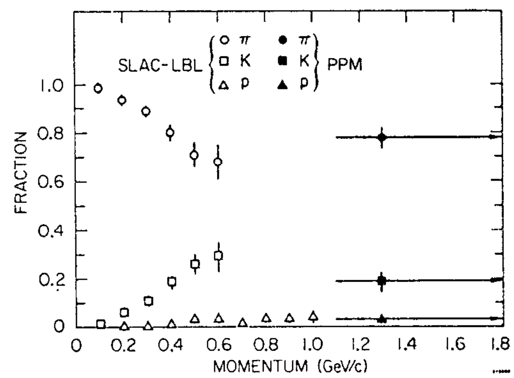

Fig. 8 The fraction of charged particles versus momentum at 4.8 GeV center-of-mass energy. Data are from both the SLAC-LBL and PPM experiments.

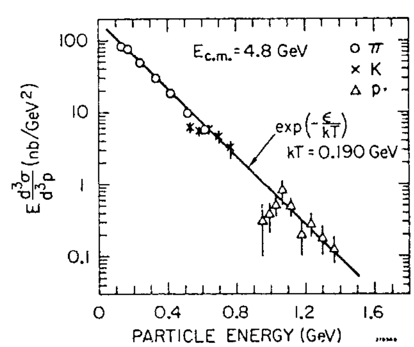

Fig. 9 Invariant cross section versus particle energy at 4.8 GeV center-of-mass energy. Data are from the SLAC-LBL experiment.

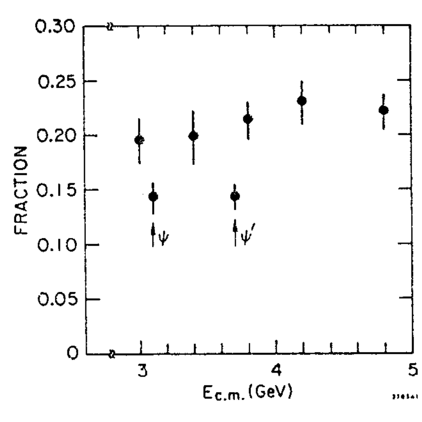

Fig. 10 Fraction of events containing a K^- with momentum less than 700 MeV/c versus center-of-mass energy.

5.3 Particle ratios

As we noted earlier, the SLAC-LBL detector can differentiate between different types of particles at low momenta by time of flight and the PPM experiment can do the same at high momenta by using a gas Cerenkov counter. The fraction of each type of particle as a function of momentum at 4.8 GeV for both experiments is shown in Fig. 8.[8,9] The fraction of K's rises with momentum from 0 to about 20% while the fraction of protons rises to a few percent.

Figure 9 shows the invariant cross section as a function of the particle energy. The data are roughly described by a single exponential with a temperature of 190 MeV. This dependence is not to be taken too literally - for instance, the slope through the kaon data alone is not the same as the general slope. However, it does indicate that the suppression of kaon and proton production relative to pion production is probably due more to mass than quantum numbers.

We have constructed the fraction of events which contain a K^- with momentum less than 700 MeV/c. This is not a fundamental quantity, but it is at least something the SLAC-LBL detector can try to measure. The data are shown in Fig. 10. Two points are significant: (a) There is no large increase in the K fraction as the energy increases through the step in R. (b) And there is an apparent small, but noticeable, decrease in the K fraction in both the ψ and ψ' decay.

6. SEARCHES FOR ψ' RADIATIVE DECAYS

6.1 Introduction

It has been suggested that if the ψ and ψ' are bound states of charm quarks, then other bound states should exist which the ψ' could decay into by the emission of a photon.[10] Some of these states could then decay into $\psi\gamma$, giving the sequence $\psi' \rightarrow \psi\gamma\gamma$. The most likely transitions in this scheme are shown in Fig. 11.

6.2 Search for $\psi\gamma\gamma$ cascades

We have already seen that the branching ratios for $\psi' \to \psi$ are[2,11]

$$\frac{\psi' \to \psi + \text{anything}}{\psi' \to \text{all}} = 0.57 \pm 0.08 \ , \tag{6a}$$

$$\frac{\psi' \to \psi\pi^+\pi^-}{\psi' \to \text{all}} = 0.32 \pm 0.04 \tag{6b}$$

and

$$\frac{\psi' \to \psi + \text{neutrals}}{\psi' \to \psi + \text{anything}} = 0.44 \pm 0.03 \ . \tag{6c}$$

If we take the ψ' to have $I = 0$ so that

$$\frac{\psi' \to \psi\pi^0\pi^0}{\psi' \to \psi\pi^+\pi^-} = 0.5 \ , \tag{7}$$

then, combining with Eqs. (6a) - (6c), we obtain

$$\frac{\psi' \to \psi + \text{neutrals (not } \pi^0\pi^0)}{\psi' \to \text{all}} = 0.09 \pm 0.03 \ . \tag{8}$$

To investigate these modes we subtract 3/2 of the $\psi' \to \psi\pi^+\pi^-$ spectrum from the $\psi' \to \psi$ + anything spectrum and plot the result in Fig. 12. The peak around a mass squared of 0.3 $(\text{GeV}/c^2)^2$ is evidence for the mode $\psi' \to \psi\eta$ which is observed in both the charged and neutral decay mode with a branching ratio

$$\frac{\psi' \to \psi\eta}{\psi' \to \text{all}} = 0.04 \pm 0.02 \ . \tag{9}$$

We don't know directly what the remaining events in Fig. 12 are. However there are two pieces of circumstantial evidence that they are the mode $\psi' \to \psi\gamma\gamma$:

i) This is the only mode left with reasonable quantum numbers.

ii) There are events below the $2\pi^0$ threshold at the 2.3 standard deviation level.

There is no evidence that the $\gamma\gamma$ mode goes via an intermediate state; it could be a direct electromagnetic decay. If it does go by an intermediate state, then from the allowed kinematics[12] we can set an upper limit of

$$\frac{\psi' \to \psi\gamma\gamma}{\psi' \to \text{all}} < 0.066 \text{ at the 90\% confidence level} \ . \tag{10}$$

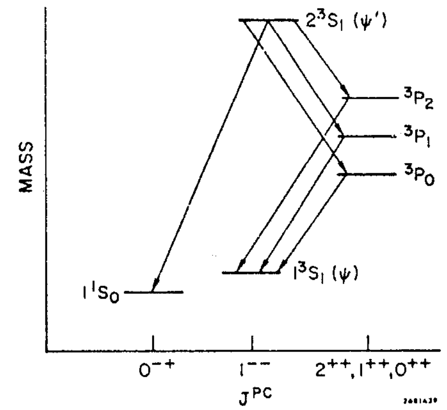

Fig. 11 The most likely gamma ray transitions in the charm model.

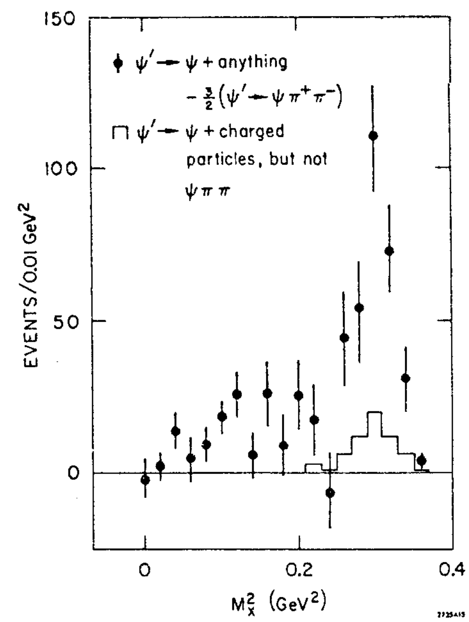

Fig. 12 The missing mass squared to the ψ corresponding to $\psi' \to \psi$ + anything - $3/2(\psi' \to \psi\pi^+\pi^-)$. The solid line indicates the missing mass squared spectrum of events in which the ψ and an additional charged particle are detected, but the detected particles are not kinematically compatible with $\psi' \to \psi\pi^+\pi^-$.

We are presently studying these $\gamma\gamma$ mode candidate events for evidence of intermediate states.

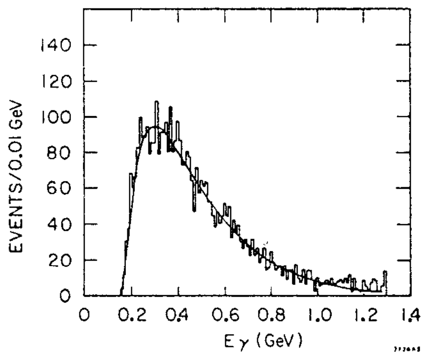

Fig. 13 Observed energy spectrum of converted photons in ψ' decays observed by the SLAC-LBL experiment. The solid line exhibits the shape of spectrum expected from π^0 decay.

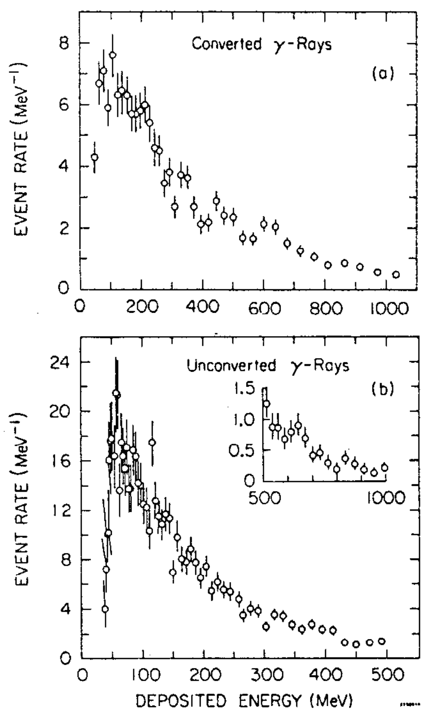

Fig. 14 Observed energy spectrum of (a) converted and (b) unconverted photons in ψ' decays observed by the Stanford experiment.

6.3 Search for monochromatic photons

Another, and more general, method of searching for intermediate states is to look for the monochromatic photons directly. Two such searches have been done, one in the SLAC-LBL magnetic detector and the other in the Stanford experiment. Neither has found significant evidence for such photons.

In the magnetic detector, the search was conducted by looking for photon conversions in the 0.052 radiation lengths of material which surround the interaction region. The observed momentum spectrum is shown in Fig. 13. The solid line represents the shape of the expected background from π^0 decay. The present analysis does not detect charged particles with momenta below 80 MeV/c and this accounts for the dropoff between 300 and 160 MeV.

In the Stanford experiment[13)] the photon energies were measured in large NaI crystals. Data are presented separately in Fig. 14 for photons which convert in lead converters in front of the crystals and for those which fail to convert. In the latter case the trigger requirements are more restrictive.

The momentum resolution and upper limits on the branching ratio B,

$$B = \frac{\psi' \to \gamma X}{\psi' \to \text{all}} \qquad (11)$$

where X is a narrow state, are given in Table 2 for both experiments.

7. SEARCH FOR NONLEPTONIC DECAYS OF CHARMED PARTICLES

We have searched for nonleptonic decays of charmed mesons with the SLAC-LBL magnetic detector by looking for narrow peaks in inclusive two and three body state invariant mass distributions in various modes.[14)] The data sample was about 10,000 hadronic events at c.m. energy 4.8 GeV. This was the largest data sample available until quite recently.

Data for a typical mode are shown in Fig. 15. This plot shows one of the two four standard deviation peaks which were observed - the bump at 2.40 GeV/c^2. (The other was at 2.05 GeV/c^2 in the $K^0_S K^\pm$ mode.) We do not consider either of these peaks significant since they could not be found in the 5.0 GeV data sample.

TABLE 2

Limits on monochromatic radiative ψ' decays

γ-ray Energy (GeV)	SLAC-LBL		Stanford			
			Converted γ's		Unconverted γ's	
	$\frac{dp}{p}$ (a)	B (b)	$\frac{dp}{p}$ (a)	B (c)	$\frac{dp}{p}$ (a)	B (c)
0.075	-	-	.075	.05	.019	.06
0.15	-	-	.047	.04	.019	.09
0.25	.03	.05	.033	.04	.019	.08
0.40	.03	.03	.025	.01	.019	.06
0.60	.03	.02	.025	.05	.019	.04
0.80	.03	.02	.025	.005	.019	.015

(a) rms resolution.

(b) Upper limit on the branching ratio at 90% confidence level.

(c) Upper limit on the branching ratio at 99% confidence level.

Upper limits have been set for eight modes and they are listed in Table 3. These limits are a factor of two to five higher than what would be expected from conventional models.[15] However, the limits are probably not stringent enough to rule out the charm model.[16]

8. EVIDENCE FOR ANOMALOUS LEPTON PRODUCTION

We have observed evidence for anomalous lepton production in the SLAC-LBL magnetic detector which cannot be explained by any conventional process.[17] The primary evidence is 24 events at $E_{c.m.} = 4.8$ GeV which appear to contain an electron and a muon, but no other visible charged or neutral particles. There are conventional processes which can yield events of this type through misidentifications, but calculations of these backgrounds give only 4 to 6 events. Various internal checks make it very unlikely that these events come from known processes.

Possible processes which could give events of this type are heavy lepton production,

$$e^+e^- \to L^+L^- \quad \begin{array}{l} L^- \to e^-\bar{\nu}_e\nu_L \\ L^+ \to \mu^+\nu_\mu\bar{\nu}_L \end{array} \qquad (12)$$

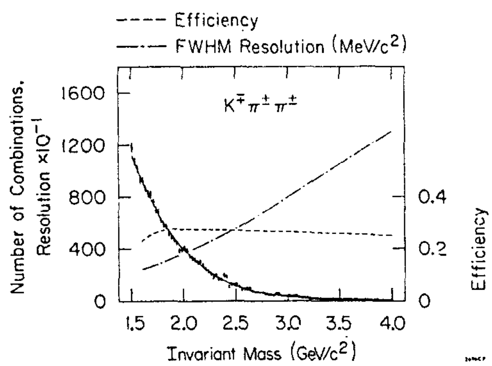

Fig. 15 Observed invariant mass distributions for $K^-\pi^+\pi^+$ and $K^+\pi^-\pi^-$ combinations. The solid line represents a smooth curve fitted to the data.

TABLE 3

Upper limits at the 90% confidence level for inclusive production cross section times branching ratio (nb)

Decay Mode	Mass Region (GeV/c^2) 1.50 to 1.85	1.85 to 2.40	2.40 to 4.00
$K^-\pi^+$ and $K^+\pi^-$	0.25	0.18	0.08
$K_S^o\pi^+\pi^-$	0.57	0.40	0.29
$\pi^+\pi^-$	0.13	0.13	0.09
K^+K^-	0.23	0.12	0.10
$K^-\pi^+\pi^+$ and $K^+\pi^-\pi^-$	0.51	0.49	0.19
$K_S^o\pi^+$ and $K_S^o\pi^-$	0.26	0.27	0.09
$K_S^oK^+$ and $K_S^oK^-$	0.54	0.33	0.09
$\pi^+\pi^-\pi^+$ and $\pi^+\pi^-\pi^-$	0.48	0.38	0.18
$K^\mp\pi^\pm$, $\bar{K}^o\pi^+\pi^-$ and $K^o\pi^+\pi^-$	1.16	0.90	0.58
K^+K^- and $\pi^+\pi^-$	0.23	0.16	0.15
$K^\mp\pi^\pm\pi^\pm$, $\bar{K}^o\pi^\pm$ and $K^o\pi^\pm$	0.64	0.51	0.30
$\bar{K}^oK^\pm$, $K^oK^\pm$ and $\pi^+\pi^-\pi^\pm$	1.10	0.76	0.29

or production of a new heavy spin one boson which decays weakly,

$$
\begin{array}{l}
e^+e^- \to M^+M^- \\
\quad\quad\quad\; \hookrightarrow e^-\bar{\nu}_e \\
\quad\quad\; \hookrightarrow \mu^+\nu_\mu \quad .
\end{array}
\tag{13}
$$

There are also other possibilities. We have not yet been able to determine which process is occurring.

Candidates for anomalous lepton production in the e^+e^- and $\mu^+\mu^-$ modes have also been observed.

The observed cross sections into the $e\mu$ mode at 4.8 GeV and several other energies are shown in Fig. 16. Corrections for geometrical and momentum cuts, which depend on the process and may be a factor of 2 to 10, have not been made.

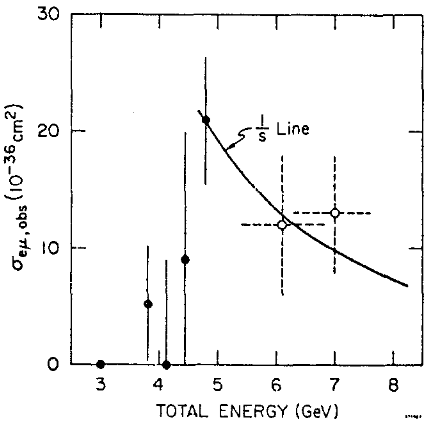

Fig. 16 The observed cross section for observing an e and a μ with no other particles in the SLAC-LBL magnetic detector. The two high energy measurements (dashed lines) are preliminary. These data have not been corrected for momentum and angle cuts and for the geometry of the detector. This correction can be a factor of 2 to 10 depending on the origin of the events.

REFERENCES

1) The present members of the SLAC-LBL collaboration are: A. M. Boyarski, M. Breidenbach, F. Bulos, G. J. Feldman, D. Fryberger, G. Hanson, D. L. Hartill, B. Jean-Marie, R. R. Larsen, D. Lüke, V. Lüth, H. L. Lynch, C. C. Morehouse, J. M. Paterson, M. L. Perl, T. P. Pun, P. A. Rapidis, B. Richter, R. F. Schwitters, W. Tanenbaum, and F. Vannucci (Stanford Linear Accelerator Center); G. S. Abrams, W. Chinowsky, C. E. Friedberg, G. Goldhaber, J. A. Kadyk, A. M. Litke, B. A. Lulu, F. M. Pierre, B. Sadoulet, G. H. Trilling, J. S. Whitaker, F. Winkelmann, and J. E. Wiss (Lawrence Berkeley Laboratory).

2) V. Lüth, invited talk at this Conference.

3) For a detailed discussion of this point see Appendix B, G. J. Feldman and M. L. Perl, Stanford Linear Accelerator Center Report No. SLAC-PUB-1615 (1975), to be published in Phys. Reports.

4.) J.-E. Augustin et al., Phys. Rev. Letters 34, 764 (1975).

5) B. Richter, Proc. of XVIIth Int. Conf. on High Energy Physics, 1974 (Science Research Council, Rutherford Laboratory, 1974).

6) A. A. Sokolov and I. M. Ternov, Sov. Phys. Doklady 8, 1203 (1964); V. N. Baier, Proc. Int. School of Physics "Enrico Fermi" (Academic Press, New York, 1971). R. F. Schwitters, Nucl. Instr. and Meth. 118, 331 (1974). U. Camerini et al., University of Pennsylvania preprint (1975).

7) F. J. Gilman, private communication.

8) C. C. Morehouse, invited talk at the April 1975 meeting of the American Physical Society, Washington, D. C.

9) T. L. Atwood et al., contribution to this Conference C-01.

10) T. Appelquist et al., Phys. Rev. Letters 34, 365 (1975); E. Eichten et al., Phys. Rev. Letters 34, 369 (1975).

11) G. S. Abrams et al., Phys. Rev. Letters 34, 1181 (1975).

12) G. J. Feldman and F. J. Gilman, SLAC Report No. SLAC-PUB-1582 (1975).

13) J. W. Simpson et al., Stanford University Report No. HEPL 759 (1975).

14) A. M. Boyarski et al., Phys. Rev. Letters 35, 196 (1975).

15) M. K. Gaillard, B. W. Lee, and J. L. Rosner, Rev. Mod. Phys. 47, 277 (1975).

16) See, for example, N. Cabbibo, invited talk at this Conference.

17) The oral version of this portion of the talk closely followed M. L. Perl, SLAC Report No. SLAC-PUB-1592 (1975), to be published in the proceedings of the Inst. of Particle Physics Summer School, McGill University, June 16-21, 1975. The reader is referred to this report for details.